HUMAN MOVEMENT (ISSN 1899-1955)
2026; 27(4): 108–119

Movement pattern and horizontal impulse responses to airflow in three trained middle-distance runners: an exploratory case series

© Wroclaw University of Health and Sport Sciences

original paper
DOI: https://doi.org/10.5114/hm/222364

SAMO RAUTER[1], BRANE ŠIROK[2], JURIJ GOSTIŠA[2], MATEUSZ JOPEK[3], KRZYSZTOF MAĆKAŁA[3], MILAN ČOH[1]

[1] Faculty of Sport, University of Ljubljana, Ljubljana, Slovenia
[2] Faculty of Mechanical Engineering, University of Ljubljana, Ljubljana, Slovenia
[3] Department of Individual and Team Physical Activities, Wroclaw University of Health and Sport Sciences, Wrocław, Poland

ABSTRACT

Purpose. This study aimed to examine, in an exploratory secondary analysis, whether signed airflow was linearly associated with horizontal impulse balance in three trained middle-distance runners and whether the accompanying multivariate movement-pattern responses were similarly organised.

Methods. Three trained male runners (22–28 years) completed one 3-min trial *per* condition in randomised athlete-specific sequences. Thirteen completed athlete-condition records covered airflow velocities of –7, –5, 0, +3, and +5 m · s^{-1}. Twenty consecutive valid steps from the final minute were averaged for each condition. A pooled within-athlete linear slope for the propulsive-to-braking impulse ratio was tested with a conditional exact randomisation procedure.

Results. The impulse ratio decreased by 0.0665 *per* 1 m · s^{-1} progression from headwind towards tailwind (95% conditional randomisation interval: –0.0819 to –0.0517; exact p = 0.000014). Individual slopes were negative in all three athletes. Propulsive impulse decreased and braking impulse increased, both associations persisting after Holm correction; temporal-spatial outcomes showed no adjusted statistical association. The response-vector analysis was exploratory and hypothesis-generating.

Conclusions. Signed airflow was associated with a directionally consistent redistribution of horizontal impulse in the three investigated athletes. These observations do not establish a population effect or a stable individual characteristic and require confirmation with repeated trials and larger samples.

Key words: air movements, biomechanical phenomena, gait analysis, athletic performance, motor activity

Introduction

Running performance emerges from the interaction between the athlete, the task, and the environment. Within this interaction, the running movement pattern can be understood as an individually organised combination of spatiotemporal, kinematic, and kinetic characteristics rather than as a single technical variable. Contemporary syntheses indicate that runners use distinct coordination strategies and that no universally optimal pattern can be prescribed independently of speed, morphology, neuromuscular capacity, experience, and external conditions [1, 2]. Kinetic and kinematic features can identify individual runners with high accuracy [3], while markedly different patterns may produce comparable running economy at endurance speeds [4]. Group summaries may therefore describe a general tendency while concealing the athlete-specific strategies through which it is achieved.

Airflow provides a controlled external constraint with which to examine such reorganisation. The aerodynamic force acting on a runner depends on the relative velocity between the body and the surrounding air, body position, and effective frontal area. Even in still air, overcoming aerodynamic resistance contributes to the mechanical demand of locomotion [5]. Classical wind-tunnel experiments quantified changes in forward motion and energetic demand during head-

Correspondence address: Krzysztof Maćkała, Department of Individual and Team Physical Activities, Wroclaw University of Health and Sport Sciences, Al. Ignacego Jana Paderewskiego 35, 51-612 Wrocław, Poland, e-mail: krzysztof.mackala@awf.wroc.pl; https://orcid.org/0000-0001-6750-4316

Received: October 07, 2026
Accepted for publication: October 22, 2026

Citation: Rauter S, Širok B, Gostiša J, Jopek M, Maćkała K, Čoh M. Movement pattern and horizontal impulse responses to airflow in three trained middle-distance runners: an exploratory case series. Hum Mov. 2026;27(4):108–119; doi: https://doi.org/10.5114/hm/222364.

wind and tailwind exposure [6, 7], and contemporary drag simulations confirm that additional horizontal resistance increases running demand [8]. The mechanical response nevertheless depends on air speed, running speed, posture, and the experimental model.

Recent wind-tunnel studies have extended this line of inquiry beyond energy expenditure. Yamashita *et al.* [9] showed that air speed and direction modified physiological and thermoregulatory responses during walking and running. Mesquita *et al.* [10] demonstrated changes in posture and the balance between positive and negative external work during headwind and tailwind exposure. In turn, Steele *et al.* [11] reported that air resistance modified braking and propulsive ground-reaction forces during treadmill running. Collectively, these findings indicate that airflow is a mechanical perturbation that must be accommodated within the runner's movement pattern, particularly through the anterior-posterior component of the ground-reaction force.

Horizontal impulse during stance directly reflects this task requirement. Air resistance can modify the braking and propulsive components of the ground-reaction force [11], whereas running speed reflects the interaction between ground-force magnitude and the time available to apply that force [12]. When a runner maintains position and speed relative to a treadmill, the propulsive and braking phases must collectively accommodate changes in external horizontal loading. However, a similar impulse balance can be achieved through different combinations of propulsive impulse, braking impulse, contact time, flight time, step frequency, and step length. A reproducible change in horizontal impulse balance therefore need not imply a single uniform temporal organisation of the step cycle.

The present study examined airflow as a task constraint on the organisation of the running movement pattern. The analysis focused on the structure of the athletes' responses across the airflow continuum. Specifically, it tested whether the balance between propulsive and braking impulses changes in a common direction within athletes and whether that functional response is achieved through a shared or athlete-specific multivariate configuration of temporal, spatial, and kinetic variables. This distinction allows a task-level mechanical response to be separated from the individual movement strategy used to produce it.

The previous report from this experiment primarily described the wind-tunnel apparatus and descriptive biomechanical responses [13]. The present secondary analysis addressed a distinct question by applying athlete-centred slopes, conditional exact randomisation tests, log-ratio and leave-one-athlete-out sensitivity analyses, and multivariate response vectors to the archived condition-level records. Its purpose was to determine whether signed airflow was associated with a pooled within-athlete linear change in horizontal impulse balance and whether movement-pattern responses were similarly organised across the three athletes. The propulsive-to-braking impulse ratio was designated as the primary outcome before the present statistical analyses began, although it was not prespecified in the original data-collection protocol. We hypothesised a negative, approximately linear association from headwind towards tailwind. Monotonic ordering was assessed descriptively, and all multivariate analyses were considered exploratory and hypothesis-generating.

Material and methods

Study design and data provenance

This study was an exploratory replicated-case analysis of biomechanical records from a controlled wind-tunnel experiment described previously [13]. The analysis was organised around athlete-specific responses: the primary estimand was a pooled within-athlete slope, and no population-average effect was assumed or inferred from the three cases.

Five airflow levels were planned: –7 and –5 m · s^{-1} (headwind), 0 m · s^{-1} (still air), and +3 and +5 m · s^{-1} (tailwind). Before testing, the five conditions were randomised separately for each athlete. Athletes completed one 3-min trial *per* condition in rotation. Each athlete then received approximately 6 min of passive recovery while the other two athletes completed their trials, and the next trial began after the athlete confirmed readiness. Athlete 1 completed all five conditions. Athletes 2 and 3 declined the fifth trial because of concurrent training demands; these were the final conditions

Table 1. Randomised airflow sequences and completed trials

Participant	Trial 1	Trial 2	Trial 3	Trial 4	Trial 5
Athlete 1	0	–7	+5	–5	+3
Athlete 2	+3	0	–5	+5	–7 not completed
Athlete 3	–5	+3	–7	0	+5 not completed

Values are signed airflow velocities in m · s^{-1}.
Negative values denote headwind, and positive values denote tailwind. The fifth scheduled condition was not completed by Athletes 2 and 3.

in their previously randomised sequences. Discontinuation was unrelated to interim biomechanical results. The dataset therefore comprised 13 completed athlete-condition records. Because each condition was measured once, trial-to-trial reproducibility and residual order or fatigue effects could not be estimated. The randomised sequences and completed trials are presented in Table 1.

Participants and ethics

Three male middle-distance runners participated. They were aged 22–28 years, and their 1500-m personal bests were closely matched (3:58.75–3:59.00). Their performance can be described as sub-elite within the Participant Classification Framework [14], although the more conservative term 'trained' is used in the title.

All participants were adults competing in the senior/open category. Athlete 2 was 22 years old and also fell within the under-23 age category; Athletes 1 and 3 were 26 and 28 years old, respectively. No participant reported a current musculoskeletal injury. The procedures and potential risks were explained before written informed consent was obtained. Participant characteristics and performance levels are presented in Table 2.

Table 2. Participant characteristics and descriptive competitive level

Participant	Age (years)	Age category	Height (cm)	Mass (kg)	1500-m personal best
Athlete 1	26	senior/open	171	58	3:59.00
Athlete 2	22	U23/open	186	72	3:58.75
Athlete 3	28	senior/open	183	74	3:58.80

Wind tunnel and airflow control

Testing was performed in the horizontal section of the closed-circuit wind tunnel at the Planica Nordic Centre, Slovenia. The horizontal section had a cross-sectional area of 10.5 m² and a nominal volume flow rate of 124 $m^3 \cdot s^{-1}$ [13]. Local airflow velocity was measured with a Schiltknecht MiniAir 20 anemometer (Schiltknecht Messtechnik AG, Gossau, Switzerland), positioned 1 m upstream of the treadmill entry in the airflow direction and on the longitudinal axis of the treadmill. The reported uncertainty between measured and nominal velocity was within approximately ± 2%.

An Assault AirRunner non-motorised curved treadmill (Assault Fitness, Carlsbad, CA, USA) was installed in the test section. The treadmill could be rotated by 180° about its vertical axis, allowing the runner to be exposed to airflow from the front or rear while retaining the same wind-tunnel flow direction. The analysed conditions were –7, –5, 0, +3, and +5 $m \cdot s^{-1}$.

Before experimental testing, each athlete completed a separate treadmill-familiarisation session lasting at least 15 min. During experimental trials, the athletes were instructed to maintain the displayed target velocity while using their natural running posture; posture was not externally constrained. Airflow and treadmill orientation remained fixed throughout each 3-min trial.

Instrumented treadmill and force acquisition

The treadmill was coupled to a custom two-axis force-measurement system. Four XNQ Electric load cells with a 60-kg capacity measured the vertical component, and two 100-kg load cells measured the fore-aft horizontal component; all sensors were specified as C2/C3 accuracy class. Before testing, the horizontal channels underwent multipoint calibration with several known loads applied in both horizontal directions. After the treadmill was rotated by 180°, the system was recalibrated and zeroed. Before every airflow condition, an unloaded wind-on baseline was recorded and subtracted from the horizontal-force signal to account for direct aerodynamic loading of the apparatus. Signals were acquired simultaneously at 1200 Hz and processed in LabVIEW [13].

The resultant vertical force was calculated as the sum of the four vertical channels, and the resultant horizontal force as the sum of the two horizontal channels. Vertical impulse was the time integral of vertical force over stance. Braking and propulsive impulses were obtained by integrating the magnitude of the negative and positive portions, respectively, of the fore–aft force signal over their corresponding stance phases. The present study used condition-level summaries generated with the established processing workflow [13].

Kinematic measurements

Treadmill-belt velocity was determined from markers fixed to the belt and recorded at 60 Hz with a Nikon D3000 camera (Nikon Corporation, Tokyo, Japan). A Photron mini UX100 high-speed camera (Photron, West Wycombe, UK) recorded the runner at 1000 Hz and was synchronised with force acquisition to visualise

foot contact [13]. The target belt velocity was 5.0 m · s^{-1} in every condition. Athletes viewed the velocity continuously and adjusted their pace towards an approximate target range of 5.0 ± 0.2 m · s^{-1} during the analysed segment. Actual condition means ranged from 4.793 to 5.262 m · s^{-1} and are reported with within-condition standard deviations in Table 3. Step length was derived from belt velocity and step frequency.

Data reduction

For each completed condition, the last 20 consecutive valid steps were selected from the final minute of the 3-min trial. Selection required stable belt velocity around the approximate 5.0 ± 0.2 m · s^{-1} target, a complete contact-flight cycle, and clearly identifiable braking and propulsive portions of the horizontal-force signal. Steps with abrupt velocity changes, signal artefacts, incomplete contact records, or ambiguous phase boundaries were excluded.

Table 3. Individual athlete-condition biomechanical values

Panel A. Horizontal impulses and belt velocity

Athlete	Airflow (m · s^{-1})	Braking impulse (N · s) mean ± *SD*	Propulsive impulse (N · s) mean ± *SD*	Impulse ratio	Belt velocity (m · s^{-1}) mean ± *SD*
Athlete 1	–7	16.665 ± 2.429	29.370 ± 2.205	1.762	4.924 ± 0.218
Athlete 1	–5	15.523 ± 2.911	26.829 ± 2.255	1.728	4.793 ± 0.204
Athlete 1	0	19.911 ± 3.233	29.721 ± 4.553	1.493	5.164 ± 0.336
Athlete 1	+3	20.449 ± 2.554	23.309 ± 2.050	1.140	4.961 ± 0.208
Athlete 1	+5	20.575 ± 4.488	20.517 ± 3.590	0.997	4.931 ± 0.139
Athlete 2	–5	19.872 ± 3.494	31.057 ± 3.124	1.563	5.137 ± 0.272
Athlete 2	0	20.560 ± 7.509	25.758 ± 8.246	1.253	5.049 ± 0.594
Athlete 2	+3	20.347 ± 10.397	19.787 ± 13.095	0.972	5.071 ± 0.199
Athlete 2	+5	20.062 ± 11.894	14.493 ± 16.062	0.722	5.102 ± 0.217
Athlete 3	–7	23.100 ± 1.856	35.818 ± 1.767	1.551	5.262 ± 0.137
Athlete 3	–5	27.570 ± 2.481	38.924 ± 2.241	1.412	5.068 ± 0.182
Athlete 3	0	29.154 ± 4.757	38.664 ± 6.478	1.326	5.105 ± 0.325
Athlete 3	+3	30.152 ± 2.609	28.034 ± 2.174	0.930	5.221 ± 0.250

Panel B. Temporal variables

Athlete	Airflow (m · s^{-1})	Contact time (ms) mean ± *SD*	Flight time (ms) mean ± *SD*	Step frequency (Hz) mean ± *SD*
Athlete 1	–7	182.218 ± 5.666	133.529 ± 6.396	3.168 ± 0.061
Athlete 1	–5	186.798 ± 7.419	133.947 ± 7.705	3.119 ± 0.060
Athlete 1	0	176.600 ± 8.692	133.403 ± 9.670	3.229 ± 0.096
Athlete 1	+3	183.407 ± 5.493	130.692 ± 9.984	3.187 ± 0.091
Athlete 1	+5	181.924 ± 10.294	131.473 ± 11.799	3.192 ± 0.071
Athlete 2	–5	178.109 ± 12.611	166.365 ± 13.434	2.905 ± 0.077
Athlete 2	0	212.270 ± 32.022	142.758 ± 29.017	2.820 ± 0.101
Athlete 2	+3	187.768 ± 48.427	158.159 ± 48.825	2.893 ± 0.074
Athlete 2	+5	183.345 ± 56.143	163.819 ± 56.181	2.883 ± 0.086
Athlete 3	–7	215.298 ± 9.207	119.243 ± 8.627	2.990 ± 0.057
Athlete 3	–5	203.900 ± 10.395	126.917 ± 11.391	3.024 ± 0.060
Athlete 3	0	203.110 ± 16.081	124.364 ± 15.680	3.058 ± 0.111
Athlete 3	+3	215.089 ± 8.170	113.533 ± 12.146	3.047 ± 0.117

Values are condition-level mean ± within-condition SD across the 20 accepted steps, except the impulse ratio, which was calculated from the condition-level propulsive and braking impulse means.
Negative airflow denotes headwind and positive airflow tailwind. Impulses are positive magnitudes; the ratio equals propulsive impulse divided by braking impulse.

Biomechanical variables were calculated for each accepted step and then averaged across the 20 steps to obtain one condition-level value for each athlete. The accompanying standard deviations described within-condition step variability. Individual steps were used to derive these summaries and were not treated as independent units in inferential analyses; the analytical unit was the completed athlete-condition record.

Outcome definitions and movement-pattern representation

The propulsive-to-braking horizontal impulse ratio was designated as the primary outcome before statistical analysis of the present secondary study, but it was not prespecified in the original data-collection protocol. It was calculated from positive impulse magnitudes as:

Horizontal impulse ratio = propulsive impulse / braking impulse.

Values above 1 indicate that the measured propulsive impulse exceeded the braking impulse magnitude within the summarised observation, whereas a reduction in the ratio indicates a shift towards a more balanced or relatively braking-dominant horizontal impulse profile. The ratio was chosen because it captures the functional redistribution between acceleration and deceleration phases while remaining interpretable across athletes with different absolute force magnitudes.

As a scale-robust sensitivity outcome, the natural logarithm of the impulse ratio was calculated as ln(propulsive impulse/braking impulse). On this scale, a slope can be exponentiated to express the multiplicative change in the impulse ratio *per* 1 m · s^{-1} increase in signed airflow.

Secondary movement outcomes were propulsive impulse, braking impulse, contact time, flight time, step frequency, duty factor, step length, and belt velocity. Duty factor was derived as 100 × contact time/(contact time + flight time). Step length was derived as belt velocity/step frequency. For an exploratory multivariate representation of the movement pattern, five complementary features were selected: duty factor, step frequency, step length, braking impulse, and propulsive impulse. The first three describe temporal–spatial organisation and the last two describe anterior-posterior force regulation.

Statistical analysis

Given the three-athlete sample and the athlete-specific condition coverage, conventional large-sample repeated-measures models were not used. The primary inferential analysis estimated a pooled within-athlete linear slope relating signed airflow velocity to each outcome after athlete-specific centring. For athlete *i* in condition *j*, the slope was calculated as:

$$\beta = \Sigma_i\Sigma_j (x_{ij} - \bar{x}_i)(y_{ij} - \bar{y}_i) / \Sigma_i\Sigma_j (x_{ij} - \bar{x}_i)^2$$

where: x is signed airflow velocity, y is the outcome, and $\bar{x}_i$ and $\bar{y}_i$ are the corresponding athlete-specific means. Centring removed between-athlete level differences. Accordingly, β quantified the pooled change across the observed within-athlete contrasts *per* 1 m · s^{-1} progression from headwind towards tailwind. It was not interpreted as evidence of a common population slope.

Association was evaluated with a conditional exact randomisation test [15]. Airflow order had been randomised separately for each athlete before testing. The two uncompleted trials were the final scheduled conditions and were omitted because the athletes declined further loading, not because of observed outcomes. Inference was therefore conditioned on each athlete's completed condition set: airflow labels were permuted only among that athlete's observed records while outcomes and condition counts were fixed. This approach requires exchangeability of labels within the completed set under the sharp null of no airflow association. All 5! × 4! × 4! = 69,120 allocations were enumerated, and the two-sided p value was the proportion for which $|\beta_{perm}| \geq |\beta_{observed}|$. The test assesses association in these observed athletes and does not establish population generalisability.

The horizontal impulse ratio was the single primary outcome and was not adjusted for multiplicity. The eight secondary movement outcomes were evaluated with the same exact test, and their two-sided p values were adjusted together with the Holm procedure [16]. Effect estimates and athlete-specific trajectories were emphasised over dichotomous significance decisions. Individual ordinary least-square slopes and Spearman rank correlations were calculated descriptively. For the primary outcome, Spearman correlations served as a sensitivity assessment of monotonic ordering and were not treated as independent population-level tests.

Three robustness analyses were applied to the primary result. First, the analysis was repeated for the natural logarithm of the impulse ratio. Second, raw-

and log-ratio analyses were repeated while omitting one athlete at a time. Third, a 95% conditional randomisation interval was obtained by inverting two-sided exact tests under a constant additive-slope model. This interval assumes an approximately linear, constant additive change in the centred outcome *per* 1 m · s^{-1} across the observed airflow range, with no airflow-by-order interaction. It describes design-based uncertainty for these records and is not a population confidence interval.

The movement-pattern response-vector analysis was exploratory and hypothesis-generating. Duty factor, step frequency, step length, braking impulse, and propulsive impulse were standardised within athlete, and their standardised slopes were combined into five-dimensional vectors. Mean pairwise cosine similarity quantified directional agreement and was compared with the conditional randomisation distribution from the same 69,120 allocations. Parallel analyses used a three-feature temporal-spatial vector and a two-feature horizontal-impulse vector; their three upper-tail *p* values were adjusted together with the Holm procedure. With only three athlete vectors, these analyses describe the observed cases and do not estimate a stable population structure.

Analyses were performed in Python 3.12.14 with NumPy 2.3.5, pandas 2.2.3, and SciPy 1.17.0.

Results

Thirteen athlete-condition records were analysed: two at –7 m · s^{-1}, three at –5 m · s^{-1}, three in still air, three at +3 m · s^{-1}, and two at +5 m · s^{-1}. Individual athlete-condition means and within-condition standard deviations for the main biomechanical variables are reported in Table 3. All inferential estimates refer to associations within these three observed athletes.

Primary outcome: horizontal impulse balance

The pooled within-athlete slope for the propulsive-to-braking impulse ratio was –0.0665 *per* 1 m · s^{-1} of signed airflow (95% conditional randomisation interval: –0.0819 to –0.0517; exact two-sided $p = 0.000014$). Across the observed conditions, progression from headwind towards tailwind was therefore associated with a lower impulse ratio. The interval quantifies uncertainty under the conditional randomisation model for these athletes and is not a population confidence interval.

Individual slopes were –0.0656, –0.0822, and –0.0539 *per* 1 m · s^{-1} for Athletes 1, 2, and 3, respectively. The observed condition ordering was monotonic within every athlete (Spearman $\rho = -1.00$ for each athlete). These descriptive results show directional replication across the three cases, but they do not establish the frequency or magnitude of the response in a wider runner population. Individual athlete trajectories are shown in Figure 1.

The robustness analyses produced the same directional interpretation. For the log-transformed ratio, the pooled within-athlete slope was –0.05336 *per* 1 m · s^{-1} (95% conditional randomisation interval: –0.06986 to –0.03831; exact $p = 0.000043$), corresponding to an

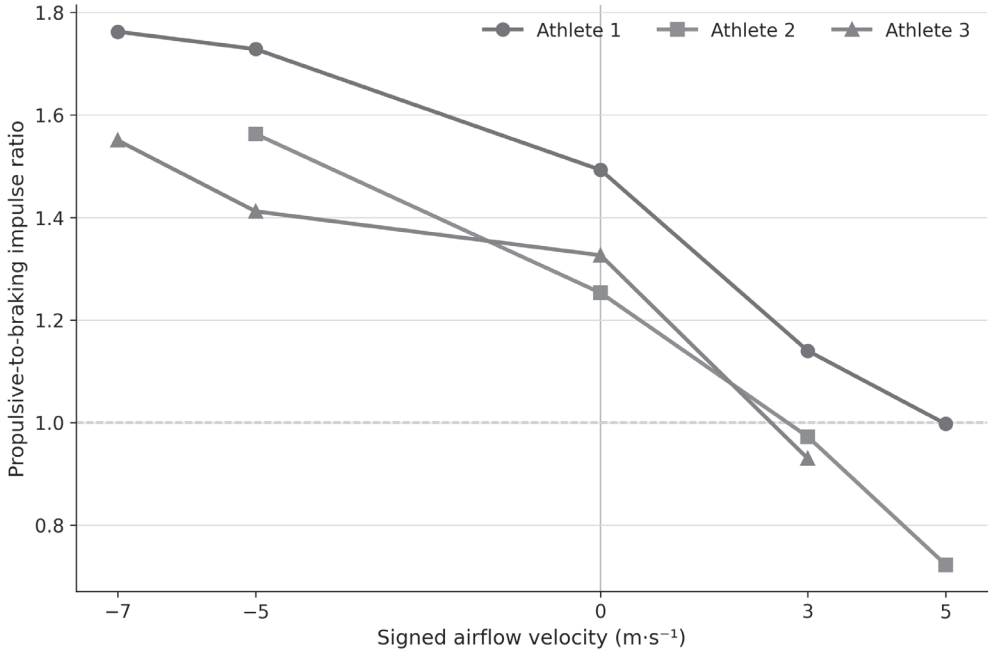


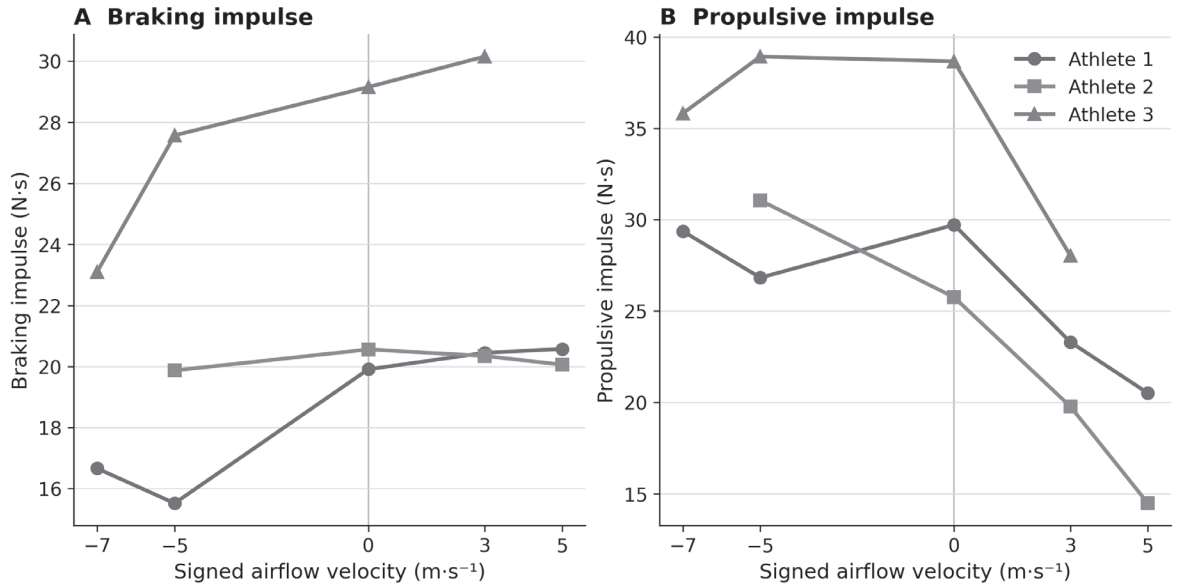
Figure 1. Individual propulsive-to-braking horizontal impulse ratios across airflow conditions Negative airflow values indicate headwind and positive values indicate tailwind. The vertical line denotes still air; the horizontal dotted line denotes equal propulsive and braking impulse magnitudes.

estimated 5.20% multiplicative decrease *per* 1 m · s^{-1}. In the leave-one-athlete-out analyses, raw-ratio slopes ranged from –0.0715 to –0.0612 and log-ratio slopes from –0.0582 to –0.0465; all remained negative.

Horizontal impulse components and secondary outcomes

The component impulses changed in complementary directions. Propulsive impulse had a pooled within-athlete slope of –0.884 N · s *per* 1 m · s^{-1} (exact p = 0.0048; Holm-adjusted p = 0.0335), whereas braking impulse magnitude had a slope of +0.375 N · s *per* 1 m · s^{-1} (exact p = 0.0020; Holm-adjusted p = 0.0161). These association tests concern the observed randomised condition assignments and should not be read as population-effect estimates. Individual braking and propulsive impulse responses are shown in Figure 2.

None of the temporal-spatial secondary outcomes showed an adjusted statistical association in the pooled within-athlete analysis. Contact time had a pooled slope of 0.001 ms *per* 1 m · s^{-1}, and all Holm-adjusted p values for contact time, flight time, step frequency, duty factor, step length, and belt velocity were 1.000. Given the three-athlete sample and one trial *per* condition, these results do not demonstrate the absence of an airflow effect or prove distinct movement strategies; they indicate only that no adjusted association was detected in the available records. Complete outcome-level results are presented in Table 4.



Impulse values are reported as positive magnitudes. Negative airflow values indicate headwind and positive values indicate tailwind; vertical lines denote still air.

Figure 2. Individual braking (A) and propulsive (B) impulses across airflow conditions

Table 4. Conditional exact randomisation tests for movement outcomes

Outcome	Pooled slope *per* 1 m · s^{-1}	Exact p	Holm-adjusted p	Status
Impulse ratio	–0.0665	0.000014	–	primary
Propulsive impulse (N · s)	–0.8837	0.005	0.034	Holm $p < 0.05$
Braking impulse (N · s)	0.3752	0.002	0.016	Holm $p < 0.05$
Contact time (ms)	0.0012	0.999	1.000	Holm $p \geq 0.05$
Flight time (ms)	–0.3375	0.463	1.000	Holm $p \geq 0.05$
Step frequency (Hz)	0.0034	0.176	1.000	Holm $p \geq 0.05$
Duty factor (pp)	0.0631	0.696	1.000	Holm $p \geq 0.05$
Step length (m)	–0.0009	0.665	1.000	Holm $p \geq 0.05$
Belt velocity (m · s^{-1})	0.0029	0.730	1.000	Holm $p \geq 0.05$

The impulse ratio was the primary outcome and was not adjusted for multiplicity. Holm correction was applied jointly to the eight secondary outcomes. Tests were conditional on each athlete's completed condition set and enumerated all 69,120 within-athlete label allocations. These tests assess association in the observed athletes, not population generalisability.

Multivariate movement-pattern analysis

The five-feature response vectors were directionally aligned in the observed cases (mean pairwise cosine similarity = 0.727; exploratory exact upper-tail p = 0.0063; Holm-adjusted p = 0.0190), with pairwise angles of 25.5°–54.2°. The horizontal-impulse vectors had a mean cosine similarity of 0.888 (exact p = 0.0372; Holm-adjusted p = 0.0744), whereas the temporal-spatial vectors had a mean cosine similarity of 0.129 (exact and Holm-adjusted p = 0.356). With only three vectors, these results are hypothesis-generating descriptions of the sampled athletes rather than evidence of a stable population pattern. The athlete-specific standardised response vectors are presented in Figure 3.

Each cell shows the within-athlete standardised slope for one feature *per* 1 m · s^{-1} progression from headwind towards tailwind. Positive values indicate an increase, negative values a decrease, and values near zero little linear change; cell shading follows the signed grey-scale key. The first three columns describe temporal-spatial organisation; the last two describe horizontal impulse. Features were standardised within athlete before slope estimation; hence, values represent direction and relative magnitude rather than original measurement units.

Discussion

Principal findings

In these three runners, signed airflow was most consistently associated with the balance of horizontal impulses rather than with a uniform temporal-spatial change. The pooled impulse-ratio slope was negative, its conditional randomisation interval excluded zero, and all individual slopes had the same direction. Propulsive impulse decreased and braking impulse increased after Holm correction. The exploratory response vectors suggested integrated directional alignment, but the sample of three athletes is insufficient to establish a stable multivariate structure or a population effect.

The observed profiles are compatible with a two-level working hypothesis. At the task level, the athletes displayed similar directional redistribution of anterior-posterior impulse. At the coordination level, they used non-identical configurations of contact time, flight time, step frequency, step length, and force variables. The findings therefore do not identify one universal running technique; they identify a candidate functional response that may be supported by more than one movement solution [1–4].

Horizontal impulse balance as a replicated within-athlete response

The clearest result concerned horizontal impulse redistribution. Wind changes the external force that must be accommodated during locomotion [5–11, 17–20], and recent treadmill evidence specifically shows modulation of horizontal ground-reaction forces by air resistance [11, 20]. It is therefore mechanically plausible that progression from headwind towards tailwind was associated with a reduced relative propulsive contribution and a greater braking contribution. The present data add directional replication across three ath-

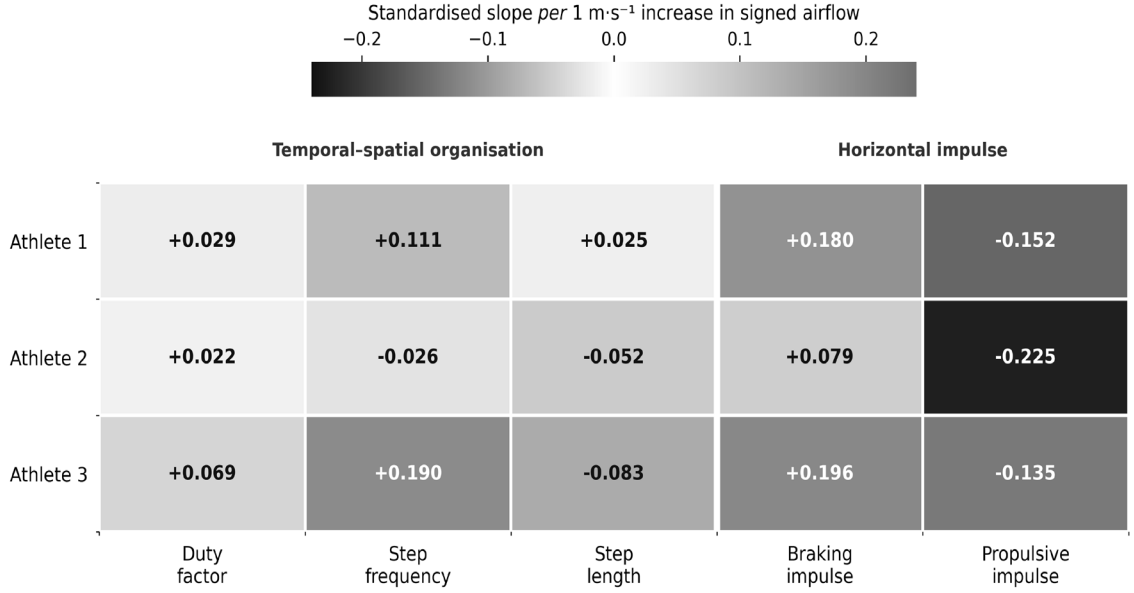


Figure 3. Athlete-specific standardised movement-pattern response vectors across signed airflow conditions

letes, but not an estimate of how common or large this response is among trained runners.

The impulse ratio should not be interpreted as a context-free score of technical quality. Braking and propulsion are coupled phases of the same step, and their values depend on belt mechanics, running speed, posture, and foot placement. In the present curved non-motorised treadmill setting, athletes regulated their position and belt speed while responding to airflow. The ratio is therefore a functional descriptor of the horizontal-force solution used in this apparatus rather than a target to maximise or minimise [1, 12, 21, 22].

The individual slopes differed in magnitude, with the steepest estimate in Athlete 2 and the shallowest in Athlete 3. These differences cannot be classified as stable responder types. Establishing an athlete-specific airflow-response characteristic would require repeated test days and explicit separation of true interindividual variation from measurement error [3, 4, 23, 24]. The log-ratio and leave-one-athlete-out analyses show that the observed association was not dependent on one scale or one athlete, but they do not add independent participants or improve population generalisability.

Observed task-level agreement and individual movement-pattern organisation

The temporal-spatial outcomes did not show adjusted statistical associations in these records. This should not be interpreted as evidence of no airflow effect or as proof that the athletes used distinct strategies. Rather, the small sample and single trial per condition leave several explanations open, including heterogeneous adjustments, limited sensitivity, and measurement variability. This pattern is also compatible with identifiable individual running signatures [3] and with evidence that no single temporal characteristic defines a universally superior technique [1, 4, 21, 22, 25].

The response-vector analysis offers a compact description but must remain secondary. Only three athlete vectors contributed to the cosine statistic. Moreover, braking and propulsive impulses are the same components used to construct the primary impulse ratio; their inclusion can therefore contribute to the observed five-feature alignment and does not constitute independent confirmation of a broader movement-pattern response. The vector findings are candidate patterns for prospective testing.

The movement-pattern perspective also cautions against treating variability or asymmetry as inherently dysfunctional. Their functional meaning depends on the task, performance level, and outcome being examined [26–28]. In airflow running, variability may reflect adaptable coordination, measurement error, or reduced control. The present records identify candidate response variables but do not justify labelling any athlete's pattern as optimal or pathological.

Practical implications

The present observations identify the horizontal impulse ratio as a candidate variable for future within-athlete monitoring, not as a validated monitoring tool. Before practical use, a protocol should standardise familiarisation, footwear, posture instructions, air speed, exposure duration, and trial order; include repeated trials and test days; and establish measurement reliability. Only then could changes in an athlete's impulse-ratio slope or accompanying movement pattern be interpreted as meaningful.

The findings do not support prescribing one universal change in contact time, step frequency, or step length. These variables should be interpreted jointly and relative to the athlete's own baseline. Body orientation and other aerodynamic factors may modify the external demand [17–20, 29], but their relationship with the movement pattern should be measured rather than assumed.

Strengths and limitations

A strength of the study is the alignment between the randomised athlete-specific condition sequences and the conditional exact randomisation analysis. The pooled slope removed between-athlete level differences, while individual trajectories, log-ratio analysis, leave-one-athlete-out checks, and a conditional randomisation interval tested the dependence of the conclusion on scale and case composition. Table 3 reports the individual condition values and within-condition variability.

The principal limitation is the number of independent participants: three athletes and 13 completed athlete-condition records cannot support population-level claims about trained or sub-elite runners. Statistical evidence against the conditional randomisation null is distinct from external validity. One trial was completed *per* condition, and the 20 steps within a trial were averaged rather than treated as independent replicates; consequently, day-to-day and trial-to-trial reliability could not be estimated. Athletes 2 and 3 stopped after four trials to limit training interference; these decisions were made independently of the interim biomechanical results, and the uncompleted airflow values were the final conditions in their previously randomised sequences.

The curved non-motorised treadmill limits transfer to overground running because belt acceleration and position regulation may contribute to the measured horizontal-force pattern [30]. The selected temporal-spatial and ground-reaction-force variables capture only part of the movement pattern; segment and joint kinematics, muscle activation, centre-of-mass motion, posture, and direct drag were not included. The response-vector analysis is exploratory relative to the sample size, and the narrowly matched adult male sample prevents assessment of sex, age, competitive level, morphology, or event specialisation as moderators.

Directions for future research

Future studies should retain randomised or counterbalanced airflow sequences while adding repeated trials and repeated test days. Hierarchical models could then estimate a population-average response, athlete-specific deviations, nonlinear effects, and residual variability while accounting for steps nested within trials and athletes. Reliability data are required before an individual slope can be interpreted as a stable movement-pattern characteristic [3, 4]. Larger samples should be stratified prospectively by sex, age category, event specialisation, and performance calibre [14].

Future measurement models should synchronise three-dimensional kinematics, ground-reaction forces, electromyography, belt dynamics, and air speed. Direct estimates of drag and frontal area would clarify whether athletes with different morphology or posture experience comparable aerodynamic demands [5, 18, 19, 29]. Such studies could test the hypothesis generated here: signed airflow may be associated with a reproducible horizontal impulse response while the supporting coordination pattern remains individually organised.

Conclusions

In the three investigated trained adult male middle-distance runners, progression from headwind towards tailwind was associated with a decrease in the propulsive-to-braking impulse ratio. Negative slopes were observed in all three cases and remained negative in the log-ratio and leave-one-athlete-out analyses. Temporal-spatial outcomes showed no adjusted statistical association, and the multivariate findings remain hypothesis-generating. The profiles cannot be considered stable individual characteristics without repeated trials and reliability assessment, and the study does not establish a population effect or one universal movement strategy.

Acknowledgements

The authors thank the athletes for their participation and Jelko Gros for enabling measurements in the Planica wind tunnel.

Data availability

Individual athlete-condition values and within-condition variability are provided in Table 3. Additional anonymised analytical data are available from the corresponding author upon reasonable request.

Ethical approval

The research related to human use complied with all the relevant national regulations and institutional policies, followed the tenets of the Declaration of Helsinki, and was approved by The Human Ethics Committee of the University of Ljubljana (approval No.: 14_2020-1442).

Informed consent

Informed consent was obtained from all individuals included in this study.

Conflict of interest

Authors state no conflict of interest.

Disclosure statement

No author has any financial interest or received any financial benefit from this research.

Funding

This research received no external funding.

References

[1] van Oeveren BT, de Ruiter CJ, Beek PJ, van Dieën JH. The biomechanics of running and running styles: a synthesis. Sports Biomech. 2024;23(4): 516–54; doi: 10.1080/14763141.2021.1873411.

[2] Gindre C, Lussiana T, Breine B, Patoz A. Mind to move: a narrative review of individualized running biomechanics beyond the spring-mass model. Sports Med. 2026;56(9):2121–38; doi: 10.1007/s40279-026-02449-w.

[3] Hoitz F, von Tscharner V, Baltich J, Nigg BM. Individuality decoded by running patterns: movement characteristics that determine the uniqueness of human running. PLOS ONE. 2021;16(4): e0249657; doi: 10.1371/journal.pone.0249657.

[4] Patoz A, Lussiana T, Breine B, Gindre C, Hébert-Losier K. There is no global running pattern more economic than another at endurance running

speeds. Int J Sports Physiol Perform. 2022;17(4): 659–62; doi: 10.1123/ijspp.2021-0345.
[5] Pecchiari MM, Legramandi MA, Gibertini G, Cavagna GA. Still air resistance during walking and running. Proc Biol Sci. 2023;290(2013);20231763; doi: 10.1098/rspb.2023.1763.
[6] Davies CTM. Effects of wind assistance and resistance on the forward motion of a runner. J Appl Physiol. 1980;48(4):702–9; doi: 10.1152/jappl.1980.48.4.702.
[7] Pugh LGCE. Oxygen intake in track and treadmill running with observations on the effect of air resistance. J Physiol. 1970;207(3):823–35; doi: 10.1113/jphysiol.1970.sp009097.
[8] da Silva ES, Kram R, Hoogkamer W. The metabolic cost of emulated aerodynamic drag forces in marathon running. J Appl Physiol. 2022;133(3): 766–76; doi: 10.1152/japplphysiol.00086.2022.
[9] Yamashita N, Ly CL, Smallcombe JW, Hodder S, Havenith G. Air speed and direction affect metabolic and thermoregulatory responses during walking and running in a temperate environment. J Appl Physiol. 2024;137(3):554–68; doi: 10.1152/japplphysiol.00159.2024.
[10] Mesquita RM, Willems PA, Catavitello G, Gibertini G, Natalucci V, Luciano F, Minetti AE, Pavei G, Dewolf AH. Biomechanics of human locomotion in the wind. J Appl Physiol. 2024;137(3):616–28; doi: 10.1152/japplphysiol.00253.2024.
[11] Steele JR, VanKeersbilck L, Bruening D, Gifford J, Seeley M, Hunter I. How oxygen uptake, ground reaction forces, and kinematics respond to air resistance and drafting during treadmill running. J Appl Biomech. 2025;41(6):511–18; doi: 10.1123/jab.2024-0316.
[12] Weyand PG, Sternlight DB, Bellizzi MJ, Wright S. Faster top running speeds are achieved with greater ground forces not more rapid leg movements. J Appl Physiol. 2000;89(5):1991–99; doi: 10.1152/jappl.2000.89.5.1991.
[13] Širok B, Gostiša J, Sečnik M, Mackala K, Čoh M. Application of wind tunnel device for evaluation of biokinetic parameters of running. Symmetry. 2021;13(3):505; doi: 10.3390/sym13030505.
[14] McKay AKA, Stellingwerff T, Smith ES, Martin DT, Mujika I, Goosey-Tolfrey VL, Sheppard J, Burke LM. Defining training and performance caliber: a participant classification framework. Int J Sports Physiol Perform. 2022;17(2):317–31; doi: 10.1123/ijspp.2021-0451.
[15] Zhang Y, Zhao Q. What is a randomization test? J Am Stat Assoc. 2023;118(544):2928–42; doi: 10.1080/01621459.2023.2199814.
[16] Holm S. A simple sequentially rejective multiple test procedure. Scand J Stat. 1979;6(2):65–70.
[17] Beaumont F, Polidori G. Aerodynamic challenges in running: understanding headwind and tailwind effects. Int J Sports Sci Coach. 2025;20(3): 1259–67; doi: 10.1177/17479541251333944.
[18] Forte P, Sousa N, Teixeira J, Marinho D, Monteiro A, Bragada J, Morais J, Barbosa T. Aerodynamic analysis of human walking, running and sprinting by numerical simulations. Acta Bioeng Biomech. 2022;24(3):3–11; doi: 10.37190/ABB-02019-2022-06.
[19] Inoue T, Okayama T, Teraoka T, Maeno S, Hirata K. Wind-tunnel experiment on aerodynamic characteristics of a runner using a moving-belt system. Cogent Eng. 2016;3(1):1231389; doi: 10.1080/23311916.2016.1231389.
[20] Steele JR, VanKeersbilck L, Hunter I. Air resistance modulates horizontal ground reaction forces during treadmill running. J Biomech. 2025;193: 113014; doi: 10.1016/j.jbiomech.2025.113014.
[21] Moore IS. Is there an economical running technique? A review of modifiable biomechanical factors affecting running economy. Sports Med. 2016; 46(6):793–807; doi: 10.1007/s40279-016-0474-4.
[22] Folland JP, Allen SJ, Black MI, Handsaker JC, Forrester SE. Running technique is an important component of running economy and performance. Med Sci Sports Exerc. 2017;49(7):1412–23; doi: 10.1249/MSS.0000000000001245.
[23] Ross R, Goodpaster BH, Koch LG, Sarzynski MA, Kohrt WM, Johannsen NM, Skinner JS, Castro A, Irving BA, Noland RC, Sparks LM, Spielmann G, Day AG, Pitsch W, Hopkins WG, Bouchard C. Precision exercise medicine: understanding exercise response variability. Br J Sports Med. 2019; 53(18):1141–53; doi: 10.1136/bjsports-2018-100328.
[24] Atkinson G, Batterham AM. True and false interindividual differences in the physiological response to an intervention. Exp Physiol. 2015;100(6): 577–88; doi: 10.1113/EP085070.
[25] Tanji F, Ohnuma H, Ando R, Yamanaka R, Ikeda T, Suzuki Y. Longer ground contact time is related to a superior running economy in highly trained distance runners. J Strength Cond Res. 2024;38(5):985–90; doi: 10.1519/JSC.0000000000000473.
[26] Krzysztofik M, Jopek M, Mroczek D, Matusiński A, Zając A. Sprint performance following plyometric conditioning activity in elite sprinters. Balt J Health Phys Act. 2024;16(1):7; doi: 10.29359/BJHPA.16.1.07.

[27] Jopek M, Krzysztofik M, Mroczek D, Zajac A, Mackala K. The influence of functional kinematic asymmetry on maximum speed performance in repeated sprints. Biol Sport. 2026;43:911–19; doi: 10.5114/biolsport.2026.158304.
[28] Jopek M, Krzysztofik M, Mroczek D, Zajac A, Mackala K. Variability of the sprint step movement pattern and its association with hamstring injury risk. J Clin Med. 2026;15(1):281; doi: 10.3390/jcm15010281.
[29] Saga N, Sanada J, Saga T, Satoh T. Aerodynamic characteristics of runners in long-distance running with platooning. Meas Sens. 2025;38(Suppl.): 101853; doi: 10.1016/j.measen.2025.101853.
[30] Van Hooren B, Fuller JT, Buckley JD, Miller JR, Sewell K, Rao G, Barton C, Bishop C, Willy RW. Is motorized treadmill running biomechanically comparable to overground running? A systematic review and meta-analysis of cross-over studies. Sports Med. 2020;50(4):785–13; doi: 10.1007/s40279-019-01237-z.

This is an Open Access article distributed under the terms of the Creative Commons Attribution-NonCommercial-NoDerivs (CC BY-NC-ND).